Engineering Microbiology 4 (2024) 100150

Contents lists available at ScienceDirect

Engineering Microbiology

journal homepage: www.elsevier.com/locate/engmic

Original Research Article

O-methyltransferase CbzMT catalyzes iterative 3,4-dimethylations for carbazomycin biosynthesis

Baixin Lin, Dashan Zhang, Junbo Wang, Yongjian Qiao, Jinjin Wang, Zixin Deng, Lingxin Kong*, Delin You*

State Key Laboratory of Microbial Metabolism, Joint International Research Laboratory of Metabolic and Developmental Sciences, School of Life Sciences & Biotechnology, Shanghai Jiao Tong University, Shanghai 200030, China

ARTICLE INFO

Keywords:
One-strain-many-compounds (OSMAC)
Carbazole
Carbazomycins
O-methyltransferase
Iterative methylation

ABSTRACT

Carbazomycins (**1**–**8**) are a subgroup of carbazole derivatives that contain oxygen at the C3 and C4 positions and an unusual asymmetric substitution pattern. Several of these compounds exhibit antifungal and antioxidant activities. To date, no systematic biosynthetic studies have been conducted on carbazomycins. In this study, carbazomycins A and B (**1** and **2**) were isolated from *Streptomyces luteosporeus* NRRL 2401 using a one-strain-many-compound (OSMAC)-guided natural product mining screen. A biosynthetic gene cluster (BGC) was identified, and possible biosynthetic pathways for **1** and **2** were proposed. The *in vivo* genetic manipulation of the O-methyltransferase-encoding gene *cbzMT* proved indispensable for **1** and **2** biosynthesis. Size exclusion chromatography indicated that CbzMT was active as a dimer. *In vitro* biochemical assays confirmed that CbzMT could repeatedly act on the hydroxyl groups at C3 and C4, producing monomethylated **2** and dimethylated **1**. Monomethylated carbazomycin B (**2**) is not easily methylated; however, CbzMT seemingly prefers the dimethylation of the dihydroxyl substrate (**12**) to **1**, even with a low conversion efficiency. These findings not only improve the understanding of carbazomycin biosynthesis but also expand the inventory of OMT-catalyzing iterative methylations on different acceptor sites, paving the way for engineering biocatalysts to synthesize new active carbazomycin derivatives.

1. Introduction

Carbazomycins (**1**–**8**) (Fig. 1A) are a subgroup of carbazoles with characteristic tricyclic systems that contain oxygen atoms at their C3 and C4 positions. They are characterized by an unusual asymmetric substitution pattern in which only one aromatic ring (ring A) is fully substituted with electron-donating substituents [1]. Among them, carbazomycin A (**1**) and carbazomycin B (**2**) were the first antibiotics of this class isolated from *Streptomyces*. They mainly inhibit the growth of phytopathogenic fungi and show weak antibacterial and anti-yeast activities [2,3]. Carbazomycin B is also active against malaria parasite *Plasmodium falciparum* [4]. Carbazomycins C–H (**3**–**9**), which possess different substituents surrounding their carbazole nuclei or carbazole-1,4-quinol frameworks, were isolated from *Streptomyces and Streptoverticillium* species [5–7]. They show moderate activity against specific fungi [6,7] and possess anti-inflammatory, antimalarial, and antituberculosis activities [5,8]. Moreover, **2** has potent radical-scavenging activity, whereas compound **1** was less effective than **2** in the *in vitro* antioxidant activity assay. However, **1** and **2** showed comparable activity in an *ex vivo* lipid peroxidation system in mouse blood plasma [9]. Therefore, this group of natural products comprises potent neuroprotective drug precursor [3]. Inspired by their molecular structures and broad application prospects, various strategies have been developed to synthesize carbazomycins, including **1** [10,11], **2** [12], and **7** and **8** [13,14]. However, the continuous development of more efficient, more (regio-)selective, and "greener" methodologies with higher overall yields is imperative.

Bacteria-derived carbazole metabolites, including carbazomycins, are less common than those in higher plants and fungi [15]. Moreover, the mechanisms underlying bacterial carbazomycin biosynthesis are not fully understood. Isotope-labeled feeding experiments with L-tryptophan, pyruvate (acetate), and S-adenosylmethionine confirmed the biogenesis of **2** [3,16,17] (Fig. 2A), which shares structural similarity with neocarazostatin A, from which the biosynthetic gene cluster (BGC) and biosynthetic pathway of the carbazole nucleus have been discovered

Abbreviations: ACP, acyl carrier protein; BGC, biosynthetic gene cluster; HPLC, high-pressure/performance liquid chromatography; LB, Luria-Bertani; NMR, nuclear magnetic resonance; OSMAC, one-strain-many-compound; SDR, short-chain dehydrogenase/reductase; SEC, size exclusion chromatography; SSN, sequence similarity network; TSBY, tryptic soy broth with yeast; WT, wild-type.

* Corresponding authors.
E-mail addresses: konglingxin7@sjtu.edu.cn (L. Kong), dlyou@sjtu.edu.cn (D. You).

https://doi.org/10.1016/j.engmic.2024.100150
Received 11 January 2024; Received in revised form 1 April 2024; Accepted 2 April 2024
Available online 2 April 2024

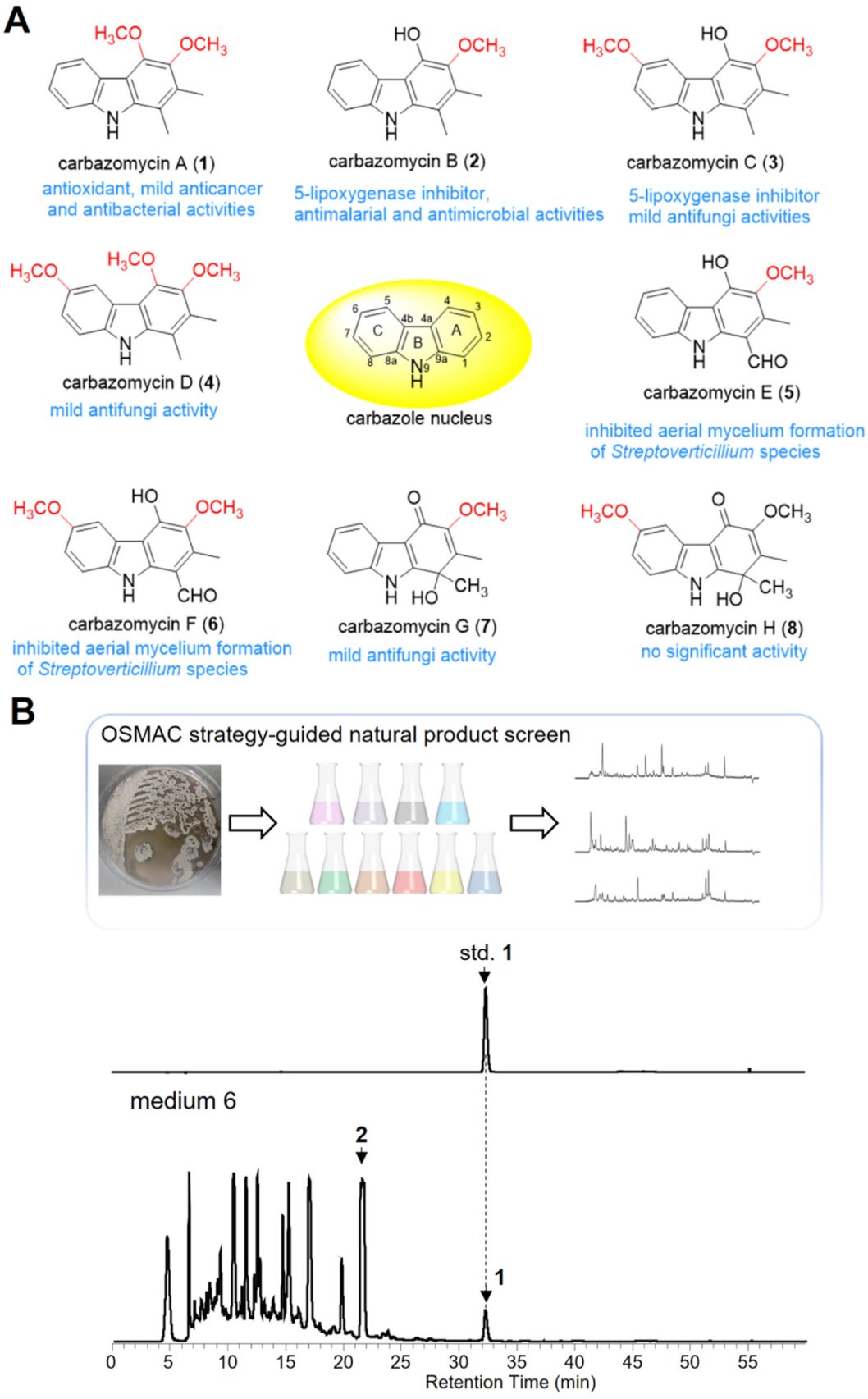

Fig. 1. Molecular structures of carbazomycins (A) and HPLC analysis of the fermentation products from medium 6 (B).

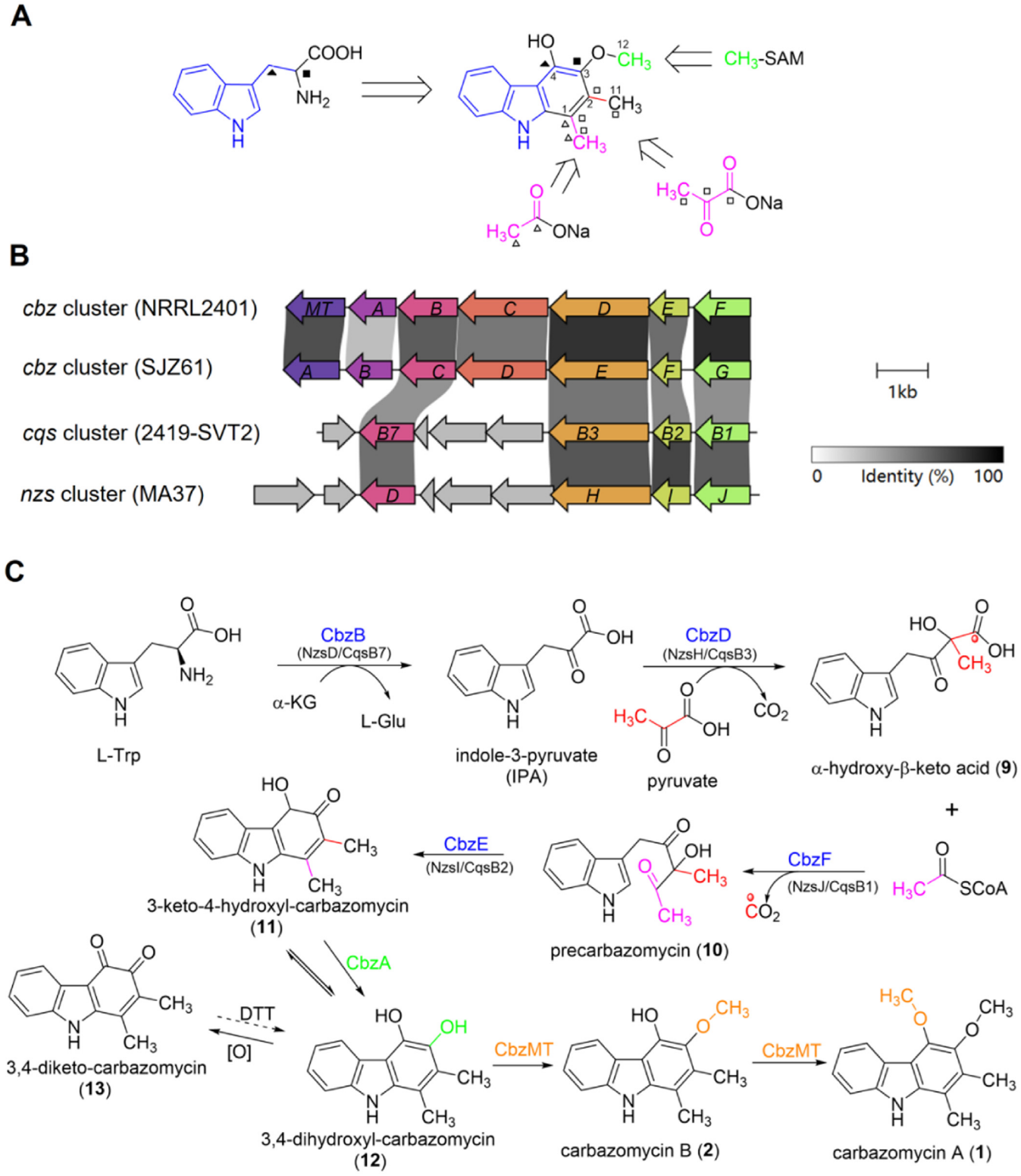

Fig. 2. Biosynthesis of carbazomycins. (A) Biogenesis of carbazomycins based on isotope-labeled precursor feeding experiments in previous studies. (B) Analysis of the *cbz* cluster and other BGCs for **2** and neocarazostatin A and carquinostatin A using the online CompArative GEne Cluster Analysis Toolbox (CAGECAT)-clinker. (C) Proposed biosynthesis process of **1** and **2**.

and characterized [15,18-20] (Fig. 2B). The reported carbazole nucleus construction mechanism appears to be common to all carbazoles, as supported by the identification of homologous proteins within a possible BGC of **2** in *Streptomyces luteoverticillatus* SZJ61 [19]. However, several aspects of this biosynthesis pathway remain unclear, including the incorporation mechanism of the two-carbon alkyl side chain in **2** rather than the four-carbon alkyl side chain in neocarazostatin A and the reduction of the carbonyl at C3 and C4 to prepare them for subsequent methylation, resulting in two methoxyl groups at C3 and C4, which are absent in neocarazostatin A.

In this study, **1** and **2** were screened from an OMSAC-guided fermentation screen of *Streptomyces luteosporeus* NRRL 2401. Their BGCs were identified, and a possible biosynthetic pathway was proposed. Based on *in vivo* genetic manipulations and *in vitro* enzymatic assays, an iterative methyltransferase, CbzMT, was shown to be responsible for the methylation of hydroxyl groups at C3, generating monomethylated **2** and the dimethylation of the hydroxyl group at C4 for the transformation of **1**. Our results fill the knowledge gap regarding the methylation process during the biosynthesis of carbazole alkaloids and provide an iterative OMT that could be developed to synthesize new carbazole derivatives.

2. Material and methods

2.1. Bacterial strains, plasmids, and growth conditions

Strains and plasmids used in this study are listed in Table S1. *Streptomyces luteosporeus* NRRL 2401 and its derivative strains were grown at 30 ˚C on solid Gauze's medium No. 1 (2 % soluble starch, 0.1 % potassium nitrate, 0.05 % sodium chloride, 0.5 % potassium phosphate dibasic, 0.5 % magnesium sulfate, 0.001 % ferrous sulfate and 1.6 % agar) for sporulation. During the OSMAC-guided screening of carbazomycins, 20 types of fermentation media were used; detailed information regarding this method is provided in Table S3. Tryptic Soy Broth with Yeast Extract (TSBY) (per liter: 3 % tryptic soy broth, 1 % yeast extract, 10.3 % sucrose, pH 7.2) was used as the seed medium and fermentation liquid medium (11 % dextrin, 1 % soluble starch, 0.25 % yeast extract, 0.5 % fine soybean powder, 0.06 % potassium phosphate dibasic, 0.1 % potassium chloride, 0.4 mg/L cobaltous chloride, pH 7.5) was used for the large-scale fermentation of carbazomycins. The *Escherichia coli* strains used for gene cloning and protein expression in this study are listed in Table S1. All strains, including DH10b, BL21 (DE3), and ET12567/pUZ8002, were grown in liquid Luria-Bertani (LB) medium or on solid LB agar plates at 37 ˚C.

2.2. DNA isolation

Briefly, 15 mL of the seed culture was collected, washed twice with an equal volume of water, and the cells were treated with lysozyme (1.5 mg/mL) for 2 h. RNase A (100 mg/mL) was then added to the cell mixture to a final concentration of 10 μg/mL to remove the RNA (37 ˚C, 1 h). Next, proteinase K and SDS were added to final concentrations of 20 mg/mL and 0.5 % (w/v), respectively, and the lysate was incubated at 55 ˚C for another 6–9 h. An equal volume of DNA extraction reagent (phenol: chloroform: isoamyl alcohol, 25:24:1) was then added to the lysate to precipitate genomic DNA. The mixture was centrifuged at 5000 × *g*, 4 ˚C for 20 min, and the supernatant was transferred into a new centrifuge tube. Then, 5 M NaCl (final concentration, 0.2 M) and ethanol (two volumes of supernatant) were added to precipitate the DNA. Finally, the precipitated DNA was washed with 70 % ethanol, dried, and dissolved in an appropriate amount of TE buffer. The quality of the extracted DNA was analyzed using a Nanodrop 2000 spectrophotometer.

2.3. Construction of gene inactivation and complementary mutants

To construct the Δ*cbzMT* mutant, the 1050-bp DNA fragment covering the *cbzMT* gene was replaced with an *aac(3)IV* + *oriT* cassette (apramycin resistant gene), which was amplified from the plasmid pIJ773 using the primers cbz-apr-P1 and cbz-apr-P2 (Table S2). Using the primers cbz-left-P1/P2 and cbz-right-P1/P2, two homologous arms flanking *cbzMT*, 1950 and 2258 bp long each, were amplified from the genomic DNA of the wild-type (WT) strain. All PCR products were cloned into *Bam*HI/*Eco*RI-digested pJTU1278 using a one-step cloning kit (Vazyme Biotech Co., Ltd., Nanjing, China) to generate the recombinant plasmid pLBX01. pLBX01 was transferred into *E. coli* ET12567/pUZ8002 and introduced into *Streptomyces luteosporeus* NRRL2401 via intergeneric conjugation [21]. The double-crossover strain Δ*cbzMT* was obtained from antibiotic selection and confirmed via PCR verification using primers cbz-test-P1 and cbz-test-P2 (Table S2).

As for the complementary strain Δ*cbzMT::cbzMT*, a 1098-bp long DNA fragment covering the intact *cbzMT* gene was amplified via PCR using primers cbz-824-P1 and cbz-824-P2 (Table S2). According to previously described methods [22], the PCR product was cloned into the *Nde*I/*Eco*RI-digested pJTU824 plasmid to generate the recombinant vector pLBX02. The resulting plasmid was introduced into the Δ*cbzMT* mutant strain via conjugation, the positive mutants were selected using thiostrepton, and then verified via PCR using the primers 824YZ-P1 and 824YZ-P2 (Table S2).

2.4. Fermentation, isolation, and purification of carbazomycin B

Briefly, 30 μL of the spore stock was inoculated into 30 mL TSBY medium, and the culture was incubated at 30 ˚C for approximately 48 h. The seed broth was then inoculated into 50 mL fermentation medium (5 % v/v) and incubated at 30 ˚C for 7 days. A total of 5 L of fermentation broth was centrifuged to obtain the mycelia and liquid phase. The liquid phase was then extracted twice with an equal volume of ethyl acetate at 25 ˚C . The crude EtOAc extract was concentrated under reduced pressure to yield brown matter (2.5 g). The crude extract was separated on a silica gel column eluted with $CHCl_3$/Methanol (100:1 to 1:1, v/v) to obtain seven fractions (A to G). Fraction A was directly separated via semi-preparative high-pressure/performance liquid chromatography (HPLC; methanol-water: 58 %, 0–31 min, 1.5 mL/min, under a 254 nm monitor) to generate mixture 1 (20 mg). Mixture 1 was separated again via semi-preparative HPLC (acetonitrile: water: 50 %, 0–30 min, 1.5 mL/min, under a 254 nm monitor) to generate compound **2** (2 mg).

2.5. HPLC, liquid chromatography with mass spectrometry (LC-MS), and nuclear magnetic resonance (NMR) analysis

HPLC analysis was carried out on an Agilent 1260 HPLC system using an Agilent ZORBAX SB-C18 column (5 μm, 4.6 × 250 mm) and an Agilent ZORBAX SB-C18 column (5 μm, 9.4 × 250 mm), respectively. For the OSMAC screen analysis, the column was equilibrated with 10 % (v/v) solvent A (H_2O with 0.1 % formic acid) and 90 % (v/v) solvent B (methanol), developed with a linear gradient (0–25 min, from 10 % B to 50 % B, 25–45 min, from 50 % B to 100 % B), and maintained at 100 % B for 5 min. UV detection was performed at 254 nm with a flow rate of 0.5 mL/min.

For fermentation product and enzymatic product analyses, the column was equilibrated with 20 % (v/v) solvent A (H_2O with 0.1 % formic acid) and 80 % (v/v) solvent B (methanol), developed with a linear gradient (0–10 min, from 20 % B to 55 % B, 10–40 min, from 55 % B to 75 % B), and then maintained at 100 % B for 5 min. UV detection was conducted at 238 nm at a flow rate of 0.5 mL/min.

The 1D-NMR and 2D-NMR spectra were obtained on a Bruker AVANCE III 700 MHz spectrometer using tetramethylsilane (TMS) as an internal standard. HR-ESI-MS spectra were recorded on an Agilent 1290 HPLC system coupled to a 6230 TOF mass spectrometer with an electrospray ionization (ESI) source (100–1000 *m/z* mass range, positive mode).

2.6. Heterologous expression and purification of recombinant cbzMT

To overexpress *cbzMT*, we amplified the intact gene (1257 bp from the genomic DNA of *Streptomyces luteosporeus* NRRL 2401) via PCR using the primers cbzMT-28a-F and cbzMT-28a-R (Table S2). PCR was performed using Pfu DNA Polymerase (Vazyme). The amplification conditions were: initial denaturation at 94 ˚C for 10 min; 30 cycles of denaturation at 94 ˚C for 45 s, annealing at 60 ˚C for 30 s, and extension at 72 ˚C for 70 s; and gap infilling at 72 ˚C for 10 min. The ob-

tained fragment was cloned into *Eco*RI/*Nde*I-digested pET28a using a one-step cloning kit (Vazyme) to obtain the overexpression plasmid, pLBX03. Recombinant pLBX03 was verified via DNA sequencing and transformed into *E. coli* BL21 (DE3) cells. The resulting transformant was cultured in LB medium containing 50 μg/mL kanamycin at 37 ˚C until the OD_{600} reached 0.6, and protein expression was induced by adding isopropylthio-*β*-*D*-galactoside (IPTG) to a final concentration of 0.2 mM. The culture was further cultivated at 16 ˚C for 22 h, harvested via centrifugation (3500 rpm, 20 min, 4 ˚C), and resuspended in 20 mL buffer A (50 mM Tris–HCl, 300 mM NaCl, pH 8.0). To purify the 6 × His-tagged protein, the bacterial cells were lysed using a high-pressure cracker at 650 bar. Cellular debris were removed via centrifugation (15,000 rpm, 1 h). The supernatant was first filtrered using a 0.45-μm polyethersulfone (PES) membrane and loaded onto a nickel-affinity chromatography setup. Buffer B (15 mL; buffer A containing 20 mM imidazole) was used to remove nonspecifically bound proteins, and buffer C (buffer A containing 250 mM imidazole) was used to elute CbzMT. The purified protein was concentrated with centrifuge filters (Amicon), desalted using a PD-10 desalting column (GE Healthcare), and finally exchanged into buffer D (50 mM Tris–HCl,150 mM NaCl, 10 % glycerol, pH 8.0). Size exclusion chromatography (SEC) was performed using a Superdex_200_10/300_GL (GE Healthcare) at 4 ˚C equilibrated in buffer D. Next, a 1-mL aliquot of the isolated protein (10 mg/mL) was loaded onto the column and eluted at a flow rate of 0.4 mL/min. The purified protein was stored in buffer D at −80 ˚C until further analysis. Protein concentration was determined using the Bradford assay with bovine serum albumin as a standard.

2.7. CbzMT activity assay

According to the typical MTase reaction system [23], the enzyme activity assay of CbzMT was carried out in 50 mM Tris–HCl buffer (pH 8.0) containing 20 μM CbzMT, 500 μM compound **2** and 800 μM S-adenosyl methionine (AdoMet/SAM, Sigma-Aldrich), at a final volume of 200 μL. To test whether compound **2** was the intermediate of CbzMT, a 150 μM mixture of **11**–**13**, 300 μM of compound **2**, and 200 μM dithiothreitol (DTT) were mixed with 100 μM or 500 μM SAM, respectively. All reactions were carried out at 30 ˚C. After 4 h, the reaction was quenched by adding two equal volumes of EtOAc and vortexing. The resulting mixture was centrifuged at 13,000 rpm for 10 min and the supernatant was subjected to LC-MS analysis under the conditions described above. Reactions with ^{13}C-SAM were conducted in a similar manner and detected using the same method.

2.8. Bioinformatics analysis

DNA sequencing was performed using an SMRT PacBio Sequel platform. The ORFs were annotated using the RAST server (https://rast.nmpdr.org/). Functions of the deduced proteins were analyzed via alignment with homologous proteins using BLAST (http://www.ncbi.nlm.nih.gov/blast/). A sequence similarity network (SSN) was created using the EFI-Enzyme Similarity Tool [24]. Following initial calculations, the SSN was finalized with an alignment score threshold of 62. The full network was visualized in Cytoscape 3.9.0 software using the 'yFiles Organic' layout. Multiple sequence alignments were conducted using BioEdit, and a phylogenetic tree of CbzMT with other OMTs was constructed using MEGA11 software [25]. The OMTs used in this study were CbzA from *Streptomyces luteoverticillatus* (AZQ75928.1), OMTA from *Aspergil parasiticus* SRRC 163 (Q12120.1), TatM1 from *Amycolatopsis* sp. DEM30355 (UUG47307.1), ROMT from *Vitis vinifera* (ABQ02270.2), UbiG from *E. coli* (CDP70731.1), FtpM from *Aspergillus fumigatus* (KMK54314.1), St6OMT1 and St6OMT2 from *Stephania tetrandra* [26], StaMA from *Streptomyces lavendulae* (WGO49567.1), and SfmM3 from *Streptomyces lavendulae* (B0CN39).

3. Results

3.1. OSMAC-guided discovery of carbazomycins

Streptomyces are prolific producers of diverse therapeutically relevant metabolites, and their production is usually influenced by a wide variety of environmental and physiological signals [27,28]. Modern 'omics'-based technologies have revealed the genomic potential of *Streptomyces* in encoding various natural products [29]. The OSMAC approach [30] has been successfully used in large-scale cultures to discover NPs with novel skeletons [31,32]. To determine the natural product diversity of *Streptomyces luteosporeus* NRRL 2401, the OSMAC strategy was utilized through fermentation in 20 different media containing various amounts of carbon, nitrogen, and trace elements (*e.g.*, zinc, copper, and cobalt) (Table S3). Comparative HPLC analysis of the secondary metabolites was conducted, and a possible metabolic peak corresponding to carbazomycin B (2) was observed in media 6, 10, and 15, with the same retention time (40.46 min) and similar UV–Vis absorption spectra. Large-scale fermentation was then conducted using medium 6 (Fig. 1B). This peak shared similar absorption spectra with those of the standard **1**, with characteristic absorptions at 224, 244, 289, and 339 nm (Fig. S2B). LC-MS analysis of this peak yielded a molecular weight of 242.31 (*m/z*, $[M + H]^+$) (Fig. S2C). Its molecular formula was determined to be $C_{15}H_{15}NO_2$ based on high-resolution electrospray ionization mass spectrometry (HR-ESI-MS) data, with an *m/z* of 242.1172 $[M + H]^+$ (Cal. 242.1181) (Fig. S2C). Repeat rounds of fractionation between silica gel chromatography and Sephadex LH-20 column chromatography, followed by semi-preparative reversed-phase HPLC, generated 2.8 mg of compound **2**. The ^{1}H nuclear magnetic resonance (NMR) spectrum of **2** showed eight signals integrated for 15 hydrogen atoms, highlighting the presence of carbazole nuclear hydrogen atoms (four signals) and methoxy group hydrogen atoms (one signal) (Fig.S3). The ^{13}C NMR spectrum showed 15 signals: eight quaternary carbons, four C–H carbons, one O–CH3 carbon, and two C–O carbons (Fig. S4). The total ^{1}H- and ^{13}CNMR data (with a chemical shift difference of <0.3 ppm) were consistent with those reported previously for **2** [33]. Therefore, compound **2** could be carbazomycin B. Trace amounts of **1** were detected during purification. LC-MS analysis gave a molecular weight of 256.20 (*m/z*, $[M + H]^+$), while HR-ESI-MS analysis gave a molecular weight of 256.1321 (*m/z*, $[M + H]^+$) (Cal. 256.1259) (Fig. S2C). Referring to the commercially available standard carbazomycin A, this compound exhibited the same retention time, MS value, UV–Vis spectra, and LC-MS/MS fragmentation type (Fig. S2A–S2D). Thus, compound **1** was confirmed to be carbazomycin A.

3.2. Candidate BGCs and possible biosynthetic pathway of carbazomycins

Previous isotope-labeled precursor feeding experiments have revealed that L-tryptophan provides the indole moiety, C-3, and C-4 of the hexa-substituted benzene ring A, pyruvic acid gives C-2 and C-11 of the carbazole A-ring, and SAM donates the methoxyl carbon C12 (Fig. 2A). Therefore, L-tryptophan was proposed to be initiallly decarboxylated and deaminated, reacted with two molecules of pyruvate, and then methylated with methionine to complete the construction of the carbon skeleton [3,16,17].

The discovery of **1** and **2** promoted the screening of candidate BGCs using the antiSMASH framework. However, no BGC was directly identified. In 2019, a possible BGC (*cbz* cluster) for **2** was identified in the genome of *S. luteoverticillatus* SZJ61 [34] without needing any further characterization. Carbazomycins share the same carbazole nucleus with neocarazostatin A. Neocarazostatin A is another type of carbazole alkaloid that possesses both an orthoquinone function and aliphatic side chains [18]. During neocarazostatin A biosynthesis, formation of the carbazole nucleus is initiated by deamination catalyzed by the aminotransferase CqsB7 (NzsD), which converts L-tryptophan to

Table 1
Annotation of genes within the *cbz* cluster identified in this study.

Gene AA		Proposed function	Homologous proteins (identity)		
			nzs cluster	*cqs* cluster	*cbz* cluster from *S. luteoverticillatus*
*cbz*MT	350	methyltransferase	none	none	CbzA (263/332)
cbzA	280	SDR	none	none	CbzB (124/159)
cbzB	355	aminotransferase	NzsD (163/316)	CqsB7 (161/316)	CbzC (248/324)
cbzC	533	FAD binding protein	none	none	CbzE (323/449)
cbzD	591	Thp-dependent enzymes	NzsH (376/582)	CqsB3 (373/585)	CbzF (497/591)
cbzE	239	cyclase	NszI (133/210)	CqsB2 (141/207)	CbzG (154/179)
cbzF	339	3-oxoacyl-[acyl-carrier-protein] synthase, KASIII	NzsJ (183/328)	CqsB1 (181/319)	CbzH (290/337)

indole-3-pyruvate (IPA). The thiamine diphosphate (ThDP)-dependent enzyme CqsB3 (NzsH) catalyzes the acyloin condensation reaction between IPA and pyruvate, producing an α-hydroxy-β-keto acid intermediate [15]. The putative β-ketoacyl-acyl carrier protein synthase (KAS) III NzsF (CqsB5) and the discrete acyl carrier protein (ACP) NzsE (CqsB6) were proved to catalyze the decarboxylative condensation between acetyl-CoA and the NzsE-bound malonyl thioester to generate 3-hydroxybutyryl-ACP, with the help of NADPH-dependent reductase FabG [19]. CqsB1(NzsJ) was the first KASIII-like enzyme that catalyzes the decarboxylative condensation between an α-hydroxy-β-keto acid and 3-hydroxybutyryl- ACP (3-HB-ACP) to form a carbazole precursor. Finally, the cyclase CqsB2 (NzsI) completes the construction of the carbazole nuclei [20].

Using CqsB7 (NzsD) and CqsB3 (NzsH) as query sequences, a possible *cbz* cluster (8.3 Kb, seven genes; accession number: PP372565) was located in the genomic region of our strain, covering nucleotides 5,951,197–5,959,479 (Fig. 2B; Table 1). Genes *cbzB, cbzD, cbzE* and *cbzF* within the *cbz* cluster exhibited a strong resemblance in organization and amino acid sequence homology with genes within the *nzs* and *cqs* clusters involved in carbazole construction. Few differences still exist, making the biosynthesis of carbazomycins different from that of neocarazostatin A. Firstly, in the *cbz* cluster, no gene encodes the homologous discrete ACP with NzsE (CqsB6), a key enzyme that catalyzes the formation of the carbazole nucleus in neocarazostatin A. Meanwhile, no homologous NzsF (CqsB5) protein can be found in the *cbz* cluster. During oxidative cyclization in the carbazole nucleus construction assay, 3-hydroxybutyryl-CoA is also available as a substrate in carbazole biosynthesis as an alternative to 3-hydroxybutyryl-ACP [20]. Considering the structural differences between neocarazostatin A and carbazomycins at the C2 site, acetyl-CoA has been proposed as a substrate for precarbazomycin (**10**) transformation. This hypothesis is consistent with a previous feeding experiment in which the C2 alkyl side chain was derived from acetate (Fig. 2A). Another difference is that two redox proteins, CbzA and CbzC, are encoded by genes without homologous proteins in the *nzs* and *cqs* clusters. Bioinformatic analysis of CbzA showed that it belongs to the atypical short-chain dehydrogenase/reductase (SDR) family and contains the conserved TGXGXXG motif for $NAD(P)^+$ binding. CbzC was annotated as an FAD/FMN-containing dehydrogenase involved in energy production and conversion. Therefore, CbzA is likely to catalyze a quinone reduction reaction similar to 3-keto-4-hydroxylcarbazomycin (**11**). The last but still significant difference is that within the *cbz* cluster, the gene *cbzMT* encodes an OMT, which is presumably related to the formation of **2**. No methoxyl-forming gene was found at the same site in the *cqs* and *nzs* clusters of neocarazostatin A. Therefore, in the proposed biosynthetic pathway of **2** (Fig. 2C), CbzB, CbzD, CbzE, and CbzF catalyze carbazole construction, similar to neocarazostatin A. The resulting compound **11** and the spontaneously oxidized compound **13** may be reduced by CbzA, leading to the formation of 3,4-dihydroxycarbazomycin (**12**). Only one encoded OMT, CbzMT, has been proposed to catalyze methylation modifications. However, all of these proposals still await confirmation.

3.3. Bioinformatics analysis of the methyltransferase cbzMT

We conducted a bioinformatics analysis to support the proposed function of CbzMT in methylating the hydroxyl group of **1** or **2**. CbzMT (GenBank: WPS70715.1) possesses 349 amino acids, a calculated molecular weight of 38.3 kDa, and belongs to class I methyltransferases (MTases), which includes all DNA MTases, some protein MTases, and many primary and secondary metabolite MTases [35]. CbzMT shares more than 50 % amino acid sequence identity with nine other hypothetical acetylserotonin O-methyltransferases (ASMTs). The original ASMT is involved in transforming serotonin to melatonin in the tryptophan metabolic pathway in both prokaryotes and eukaryotes [36]. A SSN showed that CbzMT clustered with other known OMTs, such as POMT-7 [37], BzaC [38], and TatM1 [39] (Fig. 3). In particular, CbzMT exhibits 80 % sequence identity with OMTA, encoded by *omtA* (formerly *omt-1*), which catalyzes the methylation of sterigmatocystin (ST) and dihydrosterigmatocystin (DHST) during aflatoxin synthesis [40]. CbzMT shows 64 % sequence identity with TatM1, which is involved in tatiomicin biosynthesis [39]. CbzMT possesses a dimerization domain at its N terminal, a conserved SAM binding motif E/DXGXGXG located between the β3 and α9 within the prototypical core SAM-MT fold (Fig. S5A). The overall core SAM-MT fold incorporates alternating α-helices and β-strands topologically arranged as α-β-$(\alpha$-$\beta)_5$-β [41]. Various modifications that possibly participate in substrate binding and catalysis were found within the SAM-MT fold regions of CbzMT (Fig. S5A). The phylogenetic analysis (Fig. S5B) showed that CbzMT is closely related to other homologous OMTs that act on the hydroxyl groups of the benzene ring. CbzMT occupies the same subclade as TatM1 from *Amycolatopsis* sp. DEM30355, which is involved in tatiomicin biosynthesis [39]. It is also closely related to the OMTA from *Aspergil parasiticus* SRRC 163, which is responsible for methylation involved in aflatoxin B1 biosynthesis [42]. Among the homologous proteins, ROMT catalyzes two iterative O-methylations on the same benzene ring [43]. FtpM, another iterative OMT, catalyzes the 1,11-dimethylation of *Aspergillus fumigatus* fumaric acid amides [44]. These observations suggest a similar role for CbzMT in the methylation of one or two hydroxyl groups in dihydroxycarbazomycin (**12**).

3.4. Deciphering the in vivo function of cbzMT

To determine the *in vivo* role of CbzMT, 576 bp of the *cbzMT* gene was replaced with *aac(3)IV* (an apramycin resistance gene) (Fig. S6). LC-MS and high-resolution accurate mass spectrometry Q-TOF-MS (HR-MS) were used to analyze the fermentation products of this mutant. The Δ*cbzMT* mutant did not produce carbazomycins A and B (**1** and **2**), and only accumulated at a small amount, resulting in a new peak (Fig. 4A). The UV–Vis spectrum suggested that the compound in this peak contained carbazole nucleus-like **2** (Fig. 4B). LC-MS analysis showed that this peak has two *m/z* values of 228.58 and 226.54, corresponding to the structures of **11** (and keto-enol-tautomerized **12**) and **13**, respectively (Fig. 4C). Compound **13** has an LC-MS/MS fragmentation

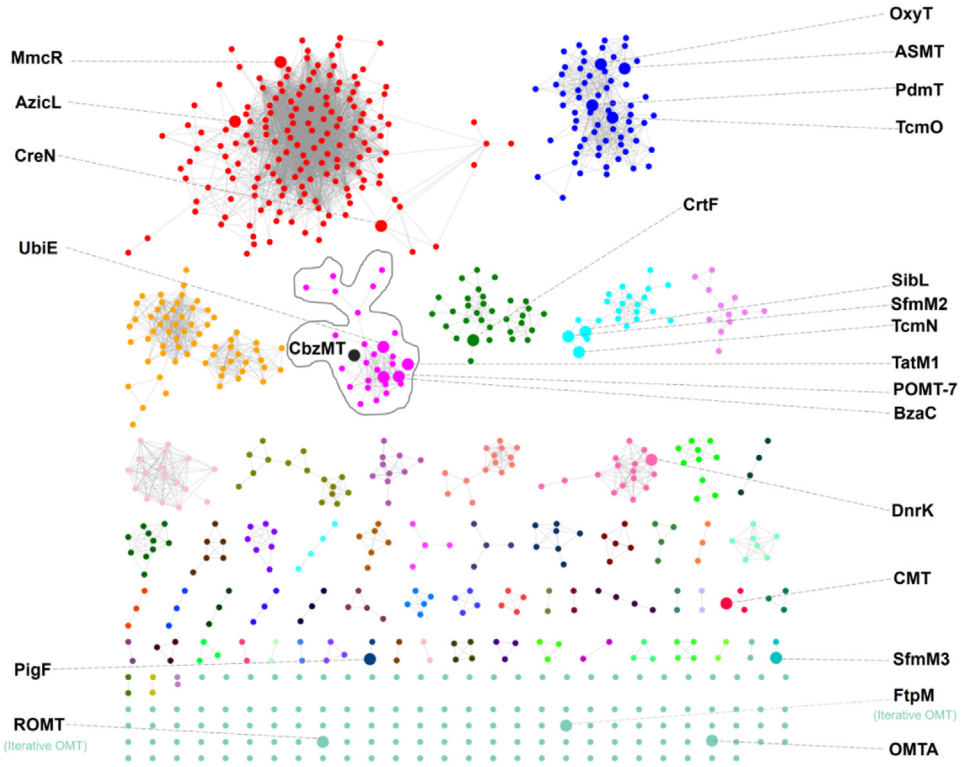

Fig. 3. Sequence similarity network (SSN) of CbzMT and its homologous proteins. OMTs with known functions are indicated. MmcR from *Planctomycetota* bacterium, AzicL from *Kibdelosporangium* sp. MJ126-NF4, CreN from *Streptomyces cremeus*, ASMT from *Burkholderiaceae* bacteria, PdmT from *Actinomadura hibisca*, TcmO from *Streptomyces glaucescens*, UbiE from *Actinomadura citrea*, TatM1 from *Amycolatopsis* sp. DEM30355, BzaC from *Actinomadura macrotermitis*, PoMT7 from *Streptomyces* sp. ADI98–10, CrtF from *Legionella moravica*, SibL from *Streptosporangium sibiricum*, SfmM2 from *Streptomyces lavendulae*, TcmN from *Amycolatopsis* sp. YIM 10, Pgm4 from *Streptomyces cirratus*, SfmM3 from *Streptomyces lavendulae*, FtpM from *Aspergillus fumigatus*, ROMT from *Vitis vinifera,* OMTA from *Aspergillus parasiticus*, and PigF from *Serratia* sp. (strain ATCC 3900).

type similar to that of **1** (Fig. S2D). Compound **11** is the keto-enol-tautomerized counterpart of **12**; **12** was easily oxidized to **13**. A similar oxidation process was observed in the CqsB1-B2-catalyzed reaction [20]. The presence of CbzA helps transform **11** into **12** *in vivo*, making the hydroxyl groups available for methylation. After the semi-preparative HPLC process, **13** changed to the predominant compound based on the HR-MS data (*m/z* 226.0867, calculated *m/z* 226.0868, molecular formula $C_{14}H_{12}NO_2$; Fig. 4D). The accumulation of these compounds suggests that CbzMT may be responsible for the methylation of the hydroxyl group at C3 of ring A at **12**. The increased production of **1** in the complementary strain Δ*cbzMT::cbzMT* confirmed the importance of this methylation (Fig. 4E). The yield of **2** in the Δ*cbzMT::cbzMT* strain was restored to approximately 40 % of the WT strain. Meanwhile, the yield of **1** in the Δ*cbzMT::cbzMT* strain was 1.9-fold higher than in the WT strain (Fig. 4F). CbzMT promoted the transformation of **2** to **1**. Based on these observations, we conclude that CbzMT may be responsible for the methylation of the hydroxyl groups at C3 and C4.

3.5. Iterative methylations catalyzed by *cbzMT*

To confirm the role of CbzMT, we expressed *cbzMT* in *E. coli* BL21(DE3)/pLysE, purified it using nickel-nitrilotriacetic acid (Ni-NTA) affinity chromatography to near homogeneity, and the purity of the resulting protein was determined using SDS-PAGE (Fig. S7A). Bioinformatics analysis suggested the presence of a dimerization domain within the CbzMT sequence. Ni-NTA-purified CbzMT was purified using SEC to determine the active form of CbzMT (Fig. S7B). CbzMT showed a peak with a retention time earlier than that of standard soybean trypsin inhibitor (STI, 29 kDa), standard ovalbumin (OVA, 43 kDa), and standard bovine serum albumin (BSA, 66 kDa) (Fig. S5B), suggesting that CbzMT exists as a dimer in solution. To determine the function of CbzMT, compound **2** was first used as the substrate in the *in vitro* enzymatic assay. As shown in Fig. 5A, CbzMT methylates **2** to produce a relatively small amount of **1**. When a mixture of compounds **11–13** (with DTT) was used as the substrate, monomethylated **2** and dimethylated **1** were produced. A mass shift of 28 Da confirmed the loading of the two methyl groups (Fig. 5B). Meanwhile, when $^{13}CH_3$-SAM was used as an alternative methyl donor, mass shifts of 1 and 2 Da were observed in the monomethylated and dimethylated products, corresponding to the incorporation of one and two labeled carbon atoms, respectively (Fig. 5C). These results indicate that CbzMT is an iterative OMT that catalyzes the methylation of two hydroxyl groups at C3 and C4 of benzene ring A during the biosynthesis of **1**.

To consolidate the findings of the *in vitro* reaction assay and to prove the occurrence of iterative methylations in the *in vivo* system, a time-course analysis of the fermentation process in the WT and Δ*cbzMT* mutant strains was conducted. In the mutant strain, the accumulation of a mixture of compounds (**11–13**) increased gradually during the fermentation process (Fig. 5Di). On the third day of fermentation, the MS value (*m/z*) of the mixture compounds (**11–13**) was dominant at 226.51 (for **13**) mixed with trace 228.59 (for **11** and **12**). On the seventh day of fermentation, a signal at 228.42 for **12** increased and exceeded that at 226.36 for **13** (Fig. 5E). This observation is consistent with the proposed role of CbzA in reducing the keto group to generate hydroxyl groups for CbzMT (Fig. 5F). In the WT strain, the amount of **1** increased gradually, but was still much lower than that of **2** (Fig. 5Dii). This observation was consistent with the fact that little **2** was transformed to **1** in the *in vitro* enzymatic reaction assay. These data suggest that the second methylation of the hydroxyl group at C4 in **2** is less likely to occur, possibly because of the preference of CbzMT for **12**. Taken together, CbzMT is one of the few characterized iterative OMTs that catalyze the 3,4-dimethylation of **12** (Fig. 5F).

4. Discussion

Carbazole is characterized as a tricyclic aromatic system composed of a central pyrrole ring fused with two benzene rings and was initially isolated from the anthracene fraction of coal tar [3]. Owing to their low redox potentials, high chemical stabilities, and facile electrophilic substitution at the C3 and C6 positions, carbazoles have attracted interest from the scientific community [45]. Many oxidized alkylated carbazoles have been isolated, and several vital active pharmaceutical in-

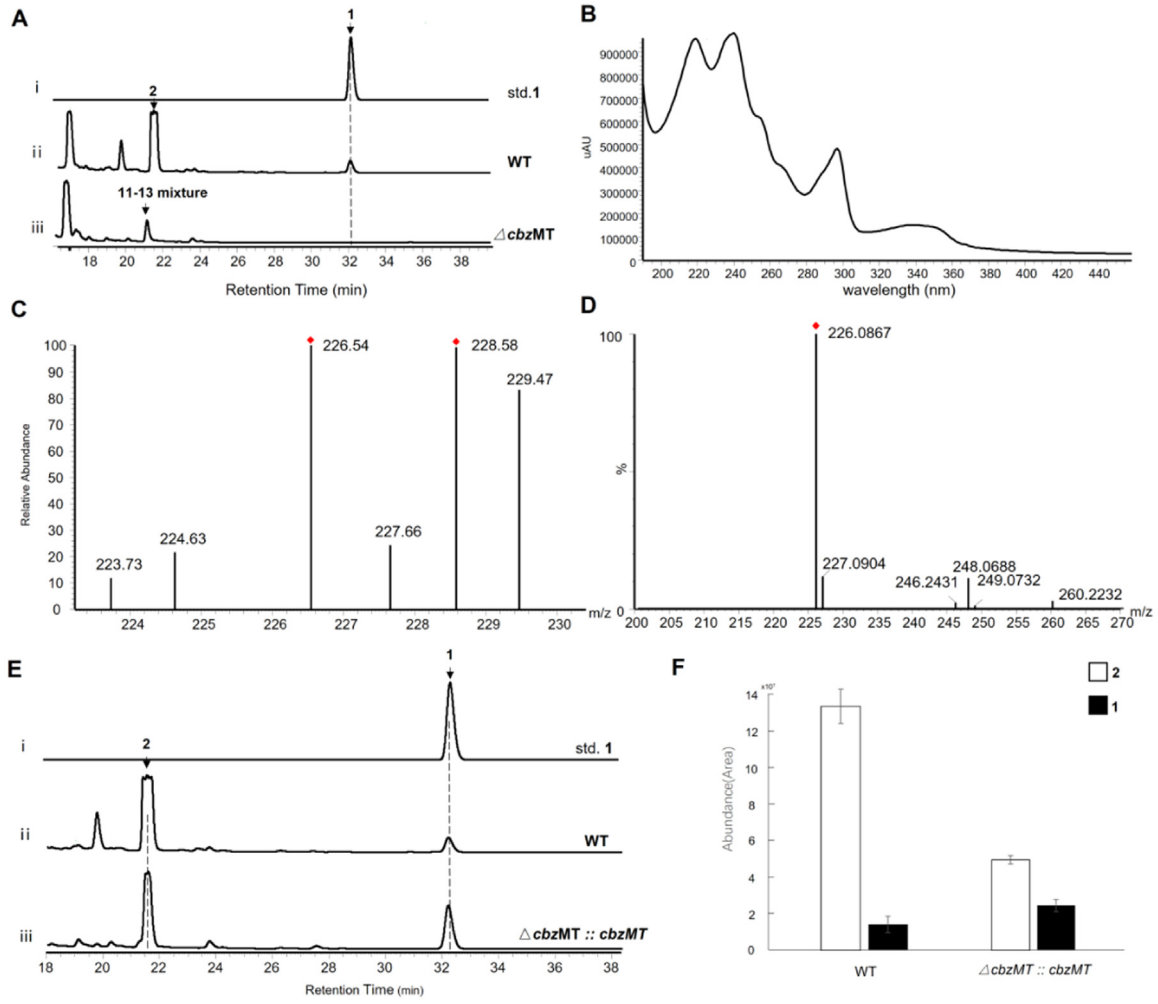

Fig. 4. *In vivo* functional study of *cbzMT*. (A) HPLC analysis of fermentation products from the WT and Δ*cbzMT* strains. (B) UV–Vis spectrum of the **11–13** mixture. (C) LC-MS analysis of the **11–13** mixture. (D) HR-MS analysis of **13**. (E-F) Quantitative analysis of **1** and **2** in the WT and Δ*cbzMT::cbzMT* strains.

gredients such as carazolol, carvedilol, and carprofen possess carbazole core structures [45,46]. Carbazomycins are a family of naturally occurring carbazoles that have a fully substituted ring A and are oxygenated at the C3 position (Fig. 1A). Several carbazomycins exhibit antifungal, antibacterial, and anticancer properties (Fig. 1A). Carbazomycins B and C display inhibitory activity against 5-lipoxygenase (IC_{50} values of 1.5 μg/mL and 1.9 mM, respectively) and are active against malaria (IC_{50} of 2.37 μg/mL against *Plasmodium falciparum*) [5]. Carbazomycin A is active against cancer (KB, MCF-7, and NCI-H187) and non-cancer (Vero) cells [5]. Many carbazomycins have been synthesized because of their biological activities and unique molecular structures. Recently, significant improvements in green synthetic methodologies for these compounds have been reported, including shorter reaction durations, performing reactions under ambient conditions, and the development of one-pot alkenylation/electrocyclization/dehydrogenation procedures [45]. More efficient and "greener" methodologies addressing selectivity and environmental shortcomings are imperative for future research endeavors.

Synthetic biology seeks interchangeable parts of natural biology to assemble systems that function in a non-natural manner [47]. Synthetic biology utilizes metabolic pathway design and genetic elements to develop organisms capable of synthesizing necessary chemicals [47]. Creating a synthetic biological system based on the manipulation of existing natural systems offers the possibility of exploiting available cellular metabolic processes, such as energy supply, protein production, and the generation of chemical precursors, to produce complex natural or non-natural products [48]. Strategies to improve the enzyme-catalyzed biosynthesis of natural products are required to mimic natural cellular processes more closely.

No systematic studies of carbazomycin biosynthesis have been reported to date. In this study, carbazomycins A and B (**1** and **2**) were isolated and purified during the OSMAC-guided screening for new active compounds (Fig. 1B), and a biosynthetic *cbz* cluster was identified. Genes involved in the biosynthesis of the carbazole nucleus showed high amino acid sequence homology with those involved in the biosynthesis of neocarazostatin A (Fig. 2). During multiple enzyme-catalyzed process, acetyl-CoA was proposed to be essential for carbazole nucleus construction, leading to the addition of a two-carbon side chain at C1. Meanwhile, an alternative pathway involving the hijacking of acetyl-ACP, catalyzed by enzymes encoded outside the *cbz* cluster, might exist. Genome retrieval identified four ACP-encoding genes. One gene, located between nucleotide positions 1,936,879 and 1,937,121, encodes a discrete FabC-like protein named CbzG. CbzG exhibited 93 % amino acid sequence identity with FabC (ACP) and possessed a conserved serine residue (Ser41). Near *cbzG*, a possible FabH-like (KSIII) protein (CbzH, 84 % sequence identity with FabH) has been identified (nucleotide positions 1,935,768–1,936,772). During fatty acid biosynthesis in *Streptomyces glaucescens*, the acetate moiety is first transferred from acetyl-CoA to acetyl-ACP (acetyl-FabC) via the transacylase activity of FabH [49]. Homologous proteins of TcmK and TcmL were also

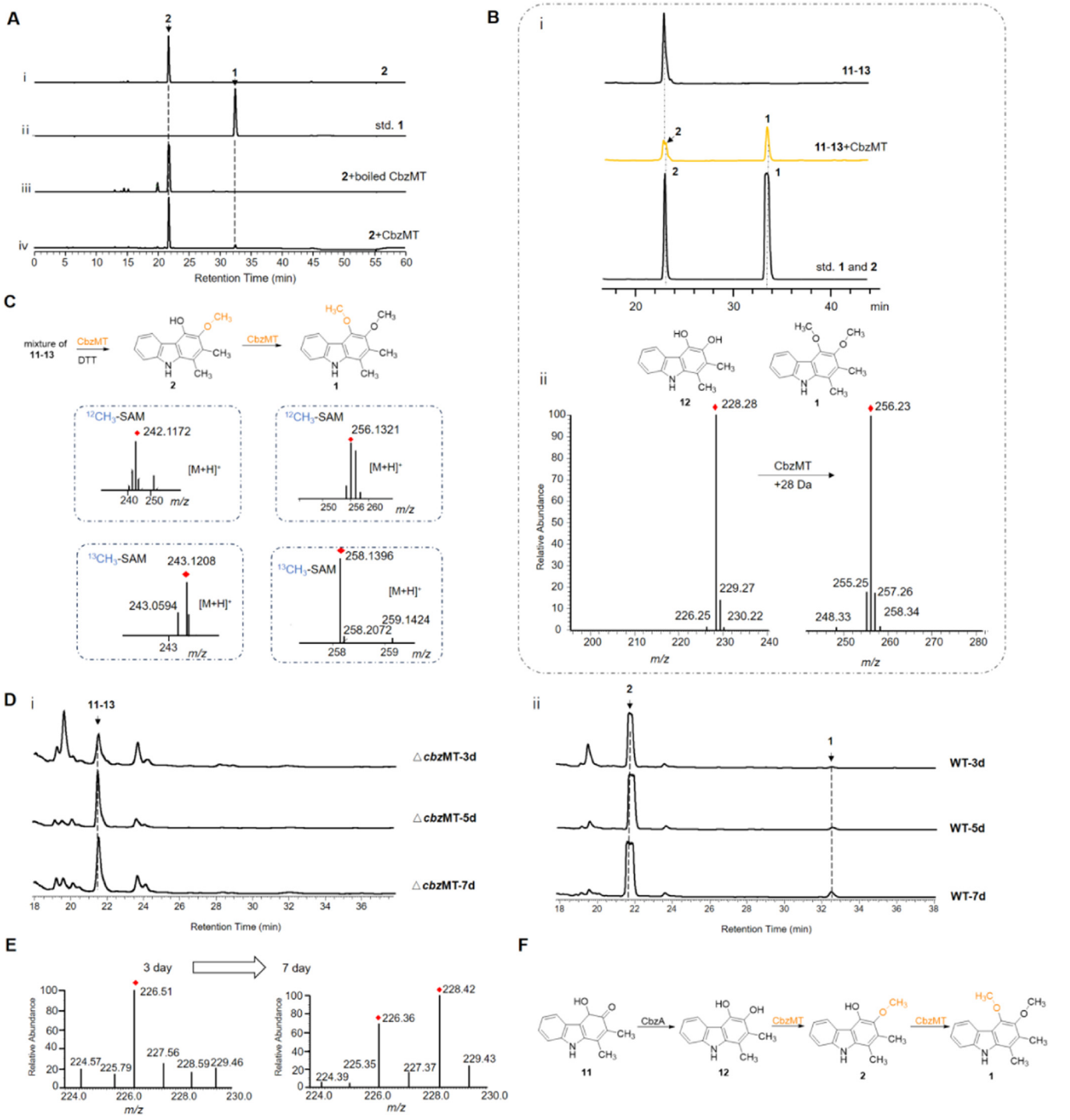

Fig. 5. Iterative methylations catalyzed by CbzMT. (A) HPLC analysis of the *in vitro* enzyme assay of CbzMT with compound **2**. (B) HPLC and LC-MS analysis of the *in vitro* enzyme assay of CbzMT with the mixture **11–13**. (C) HR-MS analysis of the *in vitro* enzyme assay using mixture **11–13** in the presence of DTT with $^{12}CH_3$-SAM and $^{13}CH_3$-SAM used as methyl donors. (D) Time-course analysis of the fermentation products of the Δ*cbzMT* and WT strains. (E) MS value analysis of mixture **11–13** during fermentation. (F) Reactions catalyzed by CbzMT.

identified, located from nucleotide positions 5,796,592 to 5,797,860 (68 % sequence identity) and from 5,797,857 to 5,799,089 (58 % sequence identity), respectively. TcmKL decarboxylates malonyl-ACP to acetyl-ACP, initiating tetracenomycin C biosynthesis [49]. These proteins have been proposed to be responsible for the addition of the two-carbon alkyl side chains at the C2 position in precarbazomycin (10) (Fig. S8). These possibilities need to be confirmed in future studies.

The hydroxyl groups at C3 and C4 are easily oxidized to the corresponding keto groups during the cyclization of the carbazole nucleus in neocarazostatin A [20]. Two genes (*cbzA* and *cbzC*) encode redox proteins, and CbzA may be responsible for the reduction of the carbonyl group at C3 *in vivo* (Fig. 2C). However, the underlying pathways remain to be elucidated. The presence of only one OMT within the *cbz* cluster suggests that CbzMT, a class I MTase, may be responsible for methylation at C3 and/or C4 in **1**. The consecutive methylation of small

molecules at the same site has been reported in the biosynthesis of mycaminose and desosamine. Both TylM1 and DesVI can catalyze the N,N-dimethylation of an amino sugar via a monomethylated intermediate in a stepwise manner [50]. PseC was biochemically characterized to catalyze the post-dimethylation of the amine group of nanangelenin [51]. Consequently, our *in vitro* assay showed that CbzMT catalyzes the iterative methylation of hydroxyl groups at these two sites, which has rarely been reported. However, the second methylation at C4 was not prone to occur in the presence of the methoxy group at C3 (Fig. 5A). To investigate whether the monomethylated **2** (300 μM) was an intermediate for CbzMT, we further tested the reaction in the presence of a mixture of **11**–**13** (150 μM) with a limiting concentration of SAM (final concentrations of 150 μM or 500 μM) (Fig. S9). In the reaction systems, the amount of **2** remained unchanged and the transformation of **1** from **11** to **13** was consistent with the supply of SAM (Fig. S9). When the Δ*cbzMT* mutant was complemented with intact *cbzMT*, more monomethylated **2** accumulated compared to monomethylated **1** (Fig. 4E). These data confirm the preference of CbzMT for non-methylated substrates (**11**–**13**), supporting the notion that monomethylated intermediates might not leave the enzyme, but might rotate inside the enzyme to be positioned for the second methylation [44]. Using the AlphaFold 2 [52] model of the CbzMT dimer, we docked **12** and **2** to rationalize the data obtained above (Fig. S10A). The pTM and pLDDT scores of the top-ranking model were 0.927 and 92.8, respectively, strongly suggesting confident prediction. The methyl donor SAM was predicted to interact with several residues in CbzMT, in good agreement with the conserved binding mode of class I MTases (Fig. S10B). The distance between the closer hydroxyl group at C3 and the methyl group of SAM was 3.35 Å. Proper positioning was ensured through hydrogen bonding with D254 (Fig. S10B). The top-ranked docking model of **12** revealed the priority for the methylation of the hydroxyl group at the C3 site, which has a slightly shorter distance to the methyl group of SAM than the hydroxyl group at the C4 site (Fig. S10C). The top-ranked docking model of **2** showed a flip of **2**, placing the hydroxyl group at C4 far from the methyl group of SAM (Fig. S10D). The second-ranked docking model of **2** gave a conformation similar to that of **12** with a small-angle rotation, placing the hydroxyl group at C4 much closer to the methyl group of SAM (Fig. S10E). All these predictions suggest that **12** could be easily methylated into **2** and that the resultant **2** remained inside the enzyme and was rotated to make the hydroxyl group at C4 easily methylated. Accordingly, the escaped **2** cannot be incorporated into the substrate pocket of CbzMT and thus can be barely be converted. However, other possible explanations cannot be excluded.

The iterative methylations catalyzed by CbzMT at different sites are reminiscent of other reported natural product OMTs, which progressively dimethylate an acceptor substrate. Plant-derived OMT (ROMT) (Fig. 3) catalyzes the formation of mono-O-methylated pinostilbene and di-O-methylated pterostilbene [43]. Another iterative OMT, FtpM (Fig. 3), repeatedly acts on the hydroxyl groups at C1 and C11 in fumaric acid amides from *Aspergillus fumigatus* in the active dimeric form [44]. Recently, FtpM has been shown to possess substrate specificity toward a range of substituted benzoic acids and exhibits potential applications in industrial biotechnology for the production of bioplastic precursors from bioderived 5-hydroxymethylfurfural [53] and poly(ethylene furanoate) plastic, potentially recycling waste plastic [54].

O-methylation is prevalent in carbazoles and methylation at different positions affects their biological activities [3,9]. The methylation of the carbazole nucleus can be used to solve the regioselectivity problem during the synthesis of carbazole alkaloids [55]. Moreover, the iterative methylation activity of CbzMT may make it a valuable biocatalyst for the transformation of more methylated carbazole derivatives.

5. Conclusion

In this study, the one-strain-many-compounds (OSMAC) strategy was used to identify the natural products of *Streptomyces luteosporeus* NRRL 2401. Carbazomycins A and B were isolated during screening. Candidate BGCs were identified, and CbzMT was shown to be responsible for the methylations of the hydroxyl groups at C3 and C4 of these two compounds. Iterative methylations at two sites catalyzed by CbzMT have rarely been reported and differ from consecutive methylations occurring at the same site of the substrate. Overall, this study facilitates the understanding of iterative OMTs and provides new materials for future applications.

Data Availability Statement

All data generated or analyzed during this study are included in this published article and its supplementary information files or are available upon request.

Declaration of Competing Interest

The authors declare that they have no known competing financial interests or personal relationships that could have appeared to influence the work reported in this paper.

CRediT Authorship Contribution Statement

Baixin Lin: Writing – original draft, Investigation, Formal analysis, Data curation. **Dashan Zhang:** Formal analysis. **Junbo Wang:** Formal analysis. **Yongjian Qiao:** Formal analysis. **Jinjin Wang:** Methodology. **Zixin Deng:** Methodology. **Lingxin Kong:** Writing – review & editing, Writing – original draft, Formal analysis. **Delin You:** Writing – review & editing, Supervision, Project administration, Conceptualization.

Acknowledgments

This work was supported by a grant from the National Key research and development Program of China (2021YFA0909500, 2021YFC2100100), and National Natural Science Foundation of China (32170077, 32170075).

Supplementary Materials

Supplementary material associated with this article can be found, in the online version, at doi:10.1016/j.engmic.2024.100150.

References

[1] P. Natho, L.A. Allen, A cyclobutanol ring-expansion approach to oxygenated carbazoles: total synthesis of glycoborine, carbazomycin A and carbazomycin B, Syn. Lett. 34 (2023) 937–942.
[2] K. Sakano, K. Ishimaru, S. Nakamura, New antibiotics, carbazomycins A and B. I. Fermentation, extraction, purification and physico-chemical and biological properties, J. Antibiot. (Tokyo). 33 (1980) 683–689.
[3] A.W. Schmidt, K.R. Reddy, H.J. Knölker, Occurrence, biogenesis, and synthesis of biologically active carbazole alkaloids, Chem. Rev. 112 (2012) 3193–3328.
[4] S. Karwehl, R. Jansen, V. Huch, M. Stadler, Sorazolons, carbazole alkaloids from *Sorangium cellulosum* strain Soce375, J. Nat. Prod. 79 (2016) 369–375.
[5] C. Intaraudom, P. Rachtawee, R. Suvannakad, P. Pittayakhajonwut, Antimalarial and antituberculosis substances from *Streptomyces* sp. BCC26924, Tetrahedron 67 (2011) 7593–7597.
[6] M. Kaneda, T. Naid, T. Kitahara, S. Nakamura, T. Hirata, T. Suga, Carbazomycins G and H, novel carbazomycin-congeners containing a quinol moiety, J. Antibiot. (Tokyo) 41 (1988) 602–608.
[7] T. Naid, T. Kitahara, M. Kaneda, S. Nakamura, C. Carbazomycins, D, E and F, minor components of the carbazomycin complex, J. Antibiot. (Tokyo) 40 (1987) 157–164.
[8] H.J. Knölker, K.R. Reddy, Isolation and synthesis of biologically active carbazole alkaloids, Chem. Rev. 102 (2002) 4303–4428.
[9] S. Kato, T. Kawasaki, T. Urata, J. Mochizuki, *In vitro* and *ex vivo* free radical scavenging activities of carazostatin, carbazomycin B and their derivatives, J. Antibiot. (Tokyo). 46 (1993) 1859–1865.
[10] S. Singh, R. Samineni, S. Pabbaraja, G. Mehta, A general carbazole synthesis via stitching of indole-ynones with nitromethanes: application to total synthesis of carbazomycin A, calothrixin B, and staurosporinone, Org. Lett. 21 (2019) 3372–3376.
[11] M. Catellani, E. Motti, N. Della Ca', New protocols for the synthesis of condensed heterocyclic rings through palladium-catalyzed aryl coupling reactions, Top. Catal. 53 (2010) 991–996.

[12] Y. Feng, T. Yukioka, M. Matsuyama, A. Mori, K. Okano, Deprotonative generation and trapping of *Haloaryllithium* in a batch reactor, Org. Lett. 25 (2023) 3013–3017.
[13] H.J. Knölker, W. Fröhner, K.R. Reddy, Iron-mediated synthesis of carbazomycin G and carbazomycin H, the first carbazole-1,4-quinol alkaloids from *Streptoverticillium ehimense*, Eur. J. Org. Chem. 2003 (2003) 740–746.
[14] Y. An, Y. Wang, X. Hu, Total synthesis of carbazomycin G by a thermal ring expansion/self-redox reaction cascade, Eur. J. Org. Chem. 2014 (2014) 3715–3718.
[15] L. Su, M. Lv, K. Kyeremeh, Z. Deng, H. Deng, Y. Yu, A ThDP-dependent enzymatic carboligation reaction involved in neocarazostatin A tricyclic carbazole formation, Org. Biomol. Chem. 14 (2016) 8679–8684.
[16] K. Yamasaki, M. KANEDA, K. WATANABE, Y. UEKI, K. ISHIMARU, S. NAKAMURA, et al., New antibiotics, carbazomycins A and B III. Taxonomy and biosynthesis, J. Antibiot. 36 (1983) 552–558.
[17] M. Kaneda, T. Kitahara, K. Yamasaki, S. Nakamura, Biosynthesis of carbazomycin B II. Origin of the whole carbon skeleton, J. Antibiot. 43 (1990) 1623–1626.
[18] S. Huang, S.S. Elsayed, M. Lv, J. Tabudravu, M.E. Rateb, R. Gyampoh, et al., Biosynthesis of neocarazostatin A reveals the sequential carbazole prenylation and hydroxylation in the tailoring Steps, Chem. Biol. 22 (2015) 1633–1642.
[19] L. Su, R. Zhang, K. Kyeremeh, Z. Deng, H. Deng, Y. Yu, Dissection of the neocarazostatin: a C4 alkyl side chain biosynthesis by *in vitro* reconstitution, Org. Biomol. Chem. 15 (2017) 3843–3848.
[20] M. Kobayashi, T. Tomita, K. Shin-ya, M. Nishiyama, T. Kuzuyama, An unprecedented cyclization mechanism in the biosynthesis of carbazole alkaloids in *Streptomyces*, Angew. Chem. Int. Ed. Engl. 58 (2019) 13349–13353.
[21] W. Zhang, L. Wang, L. Kong, T. Wang, Y. Chu, Z. Deng, et al., Unveiling the post-PKS redox tailoring steps in biosynthesis of the type II polyketide antitumor antibiotic xantholipin, Chem. Biol. 19 (2012) 422–432.
[22] J. Shen, L. Kong, Y. Li, X. Zheng, Q. Wang, W. Yang, et al., A LuxR family transcriptional regulator AniF promotes the production of anisomycin and its derivatives in *Streptomyces hygrospinosus* var. beijingensis, Synth. Syst. Biotechnol. 4 (2019) 40–48.
[23] L. Kong, Q. Wang, W. Yang, J. Shen, Y. Li, X. Zheng, et al., Three recently diverging duplicated methyltransferases exhibit substrate-dependent regioselectivity essential for xantholipin biosynthesis, ACS Chem. Biol. 15 (2020) 2107–2115.
[24] R. Zallot, N. Oberg, J.A. Gerlt, The EFI Web resource for genomic enzymology tools: leveraging protein, genome, and metagenome databases to discover novel enzymes and metabolic pathways, Biochemistry 58 (2019) 4169–4182.
[25] Y. Li, L. Kong, J. Shen, Q. Wang, Q. Liu, W. Yang, et al., Characterization of the positive SARP family regulator PieR for improving piericidin A1 production in *Streptomyces piomogeues* var. Hangzhouwanensis, Synth. Syst. Biotechnol. 4 (2019) 16–24.
[26] Q. Li, J. Bu, Y. Ma, J. Yang, Z. Hu, C. Lai, et al., Characterization of O-methyltransferases involved in the biosynthesis of tetrandrine in *Stephania tetrandra*, J. Plant. Physiol. 250 (2020).
[27] D.A. van Bergeijk, B.R. Terlouw, M.H. Medema, G.P. van Wezel, Ecology and genomics of *Actinobacteria*: new concepts for natural product discovery, Nat. Rev. Microbiol. 18 (2020) 546–558.
[28] M.J. Bibb, Regulation of secondary metabolism in *Streptomycetes*, Curr. Opin. Microbiol. 8 (2005) 208–215.
[29] K. Scherlach, C. Hertweck, Mining and unearthing hidden biosynthetic potential, Nat. Commun. 12 (2021).
[30] H.B. Bode, B. Bethe, R. Höfs, A. Zeeck, Big effects from small changes: possible ways to explore nature's chemical diversity, Chembiochem 3 (2002) 619–627.
[31] D. Zhang, J. Wang, Y. Qiao, B. Lin, Z. Deng, L. Kong, et al., Genome mining and metabolic profiling reveal cytotoxic cyclodipeptides in *Streptomyces hygrospinosus* var. Beijingensis, Antibiotics. 11 (2022).
[32] C. Wu, H.U. van der Heul, A.V. Melnik, J. Lübben, P.C. Dorrestein, A.J. Minnaard, et al., Lugdunomycin, an angucycline-derived molecule with unprecedented chemical architecture, Angew. Chem. Int. Ed. Engl. 58 (2019) 2809–2814.
[33] K.I. Sakano, S. Nakamura, New antibiotis, carbazomycins A and B II. Structural elucidation, J. Antibiot. 33 (1980) 961–966.
[34] Z. Feng, G. Chen, J. Zhang, H. Zhu, X. Yu, Y. Yin, et al., Characterization and complete genome analysis of the carbazomycin B-producing strain *Streptomyces luteoverticillatus* SZJ61, Curr. Microbiol. 76 (2019) 982–987.
[35] A.W. Struck, M.L. Thompson, L.S. Wong, J. Micklefield, S-adenosyl-methionine-dependent methyltransferases: highly versatile enzymes in bocatalysis, biosynthesis and other biotechnological applications, Chembiochem 13 (2012) 2642–2655.
[36] Y. Byeon, H.J. Lee, H.Y. Lee, K. Back, Cloning and functional characterization of the arabidopsis N-acetylserotonin O-methyltransferase responsible for melatonin synthesis, J. Pineal. Res. 60 (2016) 65–73.
[37] Y.M. Jeon, B.G. Kim, J.H. Ahn, Biological synthesis of 7-O-methyl apigenin from naringenin using *Escherichia coli* expressing two genes, J. Microbiol. Biotechnol. 19 (2009) 491–494.
[38] A.B. Hazra, A.W. Han, A.P. Mehta, K.C. Mok, V. Osadchiy, T.P. Begley, et al., Anaerobic biosynthesis of the lower ligand of vitamin B12, Proc. Natl. Acad. Sci. U. S. A. 112 (2015) 10792–10797.
[39] B. Kepplinger, L. Mardiana, J. Cowell, S. Morton-Laing, Y. Dashti, C. Wills, et al., Discovery, isolation, heterologous expression and mode-of-action studies of the antibiotic polyketide tatiomicin from *Amycolatopsis* sp. DEM30355, Sci. Rep. 12 (2022).
[40] G.A. Payne, M.P. Brown, Genetics and physiology of aflation biosynthesis, Annu. Rev. Phytopathol. 36 (1998) 329–362.
[41] J.L. Martin, F.M. McMillan, SAM (dependent) I AM: the S-adenosylmethionine-dependent methyltransferase fold, Curr. Opin. Struct. Biol. 12 (2002) 783–793.
[42] N.P. Keller, H.C. Dischinger, D. Bhatnagar, T.E. Cleveland, A.H. Ullah, Purification of a 40-kilodalton methyltransferase active in the aflatoxin biosynthetic pathway, Appl. Environ. Microbiol. 59 (1993) 479–484.
[43] N. Kallscheuer, M. Vogt, M. Bott, J. Marienhagen, Functional expression of plant-derived O-methyltransferase, flavanone 3-hydroxylase, and flavonol synthase in Corynebacterium glutamicum for production of pterostilbene, kaempferol, and quercetin, J. Biotechnol. 258 (2017) 190–196.
[44] D. Kalb, T. Heinekamp, S. Schieferdecker, M. Nett, A.A. Brakhage, D. Hoffmeister, An iterative O-methyltransferase catalyzes 1,11-dimethylation of *Aspergillus fumigatus* fumaric acid amides, Chembiochem 17 (2016) 1813–1817.
[45] L.A.T. Allen, P. Natho, Trends in carbazole synthesis-an update (2013-2023), Org. Biomol. Chem. 45 (2023) 8956–8974.
[46] L.M. Alkhalaf, K.S. Ryan, Biosynthetic manipulation of tryptophan in bacteria: pathways and mechanisms, Chem. Biol. 22 (2015) 317–328.
[47] S.A. Benner, A.M. Sismour, Synthetic biology, Nat. Rev. Genet. 6 (2005) 533–543.
[48] S. Hirschi, T.R. Ward, W.P. Meier, D.J. Müller, D. Fotiadis, Synthetic Biology: bottom-up assembly of molecular systems, Chem. Rev. 122 (2022) 16294–16328.
[49] G. Florova, G. Kazanina, K.A. Reynolds, Enzymes involved in fatty acid and polyketide biosynthesis in *Streptomyces glaucescens*: role of FabH and FabD and their acyl carrier protein specificity, Biochemistry 41 (2002) 10462–10471.
[50] H. Chen, H. Yamase, K. Murakami, C.W. Chang, L. Zhao, Z. Zhao, et al., Expression, purification, and characterization of two N,N-dimethyltransferases, TylM1 and DesVI, involved in the biosynthesis of mycaminose and desosamine, Biochemistry 41 (2002) 9165–9183.
[51] X.X. Xue, L. Chen, M.C. Tang, Genome mining discovery of a new benzazepine alkaloid pseudofisnin A from the marine fungus *Neosartorya pseudofischeri* F27-1, Antibiotics 11 (2022).
[52] J. Jumper, R. Evans, A. Pritzel, T. Green, M. Figurnov, O. Ronneberger, et al., Highly accurate protein structure prediction with AlphaFold, Nature 596 (2021) 583–589.
[53] L.C. Ward, H.V. McCue, D.J. Rigden, N.M. Kershaw, C. Ashbrook, H. Hatton, et al., Carboxyl methyltransferase catalysed formation of mono-and dimethyl esters under aqueous conditions: application in cascade biocatalysis, Angew. Chem. 134 (2022).
[54] L.C. Ward, E. Goulding, D.J. Rigden, F.E. Allan, A. Pellis, H. Hatton, et al., Engineering a carboxyl methyltransferase for the formation of a furan-based bioplastic precursor, ChemSusChem. 16 (2023).
[55] X. Zheng, L. Lv, S. Lu, W. Wang, Z. Li, Benzannulation of indoles to carbazoles and its applications for syntheses of carbazole alkaloids, Org. Lett. 16 (2014) 5156–5159.